

# Simplified Method for the Assessment of Elastic-Plastic Shakedown in Piping

Wolf Reinhardt

Reactor Engineering, Atomic Energy of Canada Limited, Mississauga ON, Canada

## ABSTRACT

The analysis for shakedown in nuclear Class 1 piping following NB-3600 of the ASME Boiler and Pressure Vessel Code (2004) contains several simplifications and can be overly conservative in some cases and potentially non-conservative in some others. A detailed elastic-plastic analysis following NB-3228.4, on the other hand, is computationally expensive and time consuming because an elastic-plastic model needs to be cycled to stabilization. A non-cyclic method to assess elastic plastic shakedown has been proposed and is applied to piping here. It requires only an analysis of a single bounding cycle to be performed. The method is used to derive the interaction diagrams for primary membrane and bending with secondary bending loads.

## INTRODUCTION

The ASME NB-3600 design rules for piping require a check for ratcheting (incremental cyclic deformation). However, the design formulas that the Code offers for this check are based on a few simple scenarios and are not strictly valid for a general piping system. As a result, in some cases of severe thermal loading, the Code assessment can be overly conservative. Some Class 1 attached piping systems with severe thermal loading were mentioned as an example in the literature [1]. It can also be shown that the Code analysis may be unconservative, although typically, the dominant moment loading and redundancies in a piping system would make such a case rare.

A non-cyclic method to demonstrate shakedown (i.e. the absence of ratcheting) was developed in [2]. This method can be applied to piping analysis, as will be demonstrated below in a few examples. The ratchet boundary in the classical Bree diagram can be re-derived with this method and analytical solutions for some other cases of interest with axially uniform loading can be established. Based on these solutions, a numerical two-step ratcheting assessment can be implemented in a finite element software.

This paper will focus on straight pipes that ratchet in a “beam mode”. The paper does not address the specifics of elements such as elbows. It will also not address the radial ratcheting of a pipe, to which NB-3653.7 “Thermal Stress Ratchet” applies. A justification of these restrictions is given in [1], where it is pointed out that the analysis of straight pipes forms the basis of the NB-3600 piping design methodology, a point that is also made in WRC Bulletin 361 [3]. Radial ratcheting of straight pipes with through-thickness thermal gradients is adequately covered in NB-3653.7. The case of radial ratchet under stresses that are not uniform around the circumference is more complicated, and is not addressed in this paper.

## ELASTIC-PLASTIC SHAKEDOWN

For a pressurized component to be acceptable to Section III, Subsection NB of the ASME Boiler and Pressure Vessel Code [4], the absence of incremental plastic straining (ratcheting) under cyclic loads must be demonstrated. The Code rules imply that the material model used in this kind of analysis should be perfectly-plastic. If such a material obeys the usual conventions of classical plasticity and a cyclic load is applied, one can show that the stresses and strain rates will undergo steady cycling after a transient period [5]. The steady response can exhibit either linearly increasing strains per cycle (ratcheting), which is prohibited by the Code, or periodic straining with or without plasticity, either of which is allowed.

The Code calls the condition where the strains are periodic during the steady cycle “shakedown”. In contrast, the classical definition of shakedown extends only to the case where the steady case is purely elastic (“elastic shakedown”). This paper adopts the wider definition of the Code, where shakedown can be either elastic or plastic, where plastic shakedown means that plasticity occurs during the steady cycle. The classical literature has established powerful theorems to address elastic shakedown. These theorems allow the calculation of upper and lower bounds to the loads for which elastic shakedown can be guaranteed. No such general theorems exist presently for plastic shakedown.

Two types of loads (or stress) are important in the evaluation of shakedown. The first are cyclic loads, which are repeated periodically and are considered as fully reversed, i.e. as going from a value of +extreme to –extreme. These loads will be considered as equivalent to loads that vary proportionally between their two extremes.

The effect of a cyclic load is that it “occupies” part of the load carrying capacity of the structure. It does not matter much whether the cyclic load is of primary or secondary type; the only difference is that the cyclic primary load might cause plastic collapse if it is high enough, whereas the secondary load cannot.

The second important type of load is a constant (not time varying) primary load, which could induce ratcheting because it “biases” the structure to deform in a certain direction. It is the contention of this paper that ratcheting is much like plastic

collapse, except that it happens incrementally whereas plastic collapse happens all at once. A more detailed discussion of ratcheting can be found in [6].

The lower bound method described in [2] is based on a generalization of Melan's [7] lower bound shakedown theorem and involves the following steps:

1. Decompose the loading into constant and fully reversed proportional components.
2. Create a finite element model of the structure under consideration. Use elastic-perfectly plastic properties with the cyclic yield stress  $\sigma_y$ . This is the initial current yield stress  $\sigma_{yc}^{(1)}$ .
3. Apply the load range of the fully reversed cyclic loading components. Obtain the stress distribution.
4. For each location (element), subtract one half of the von Mises equivalent stress range defined by eq. (1) from the current yield stress  $\sigma_{yc}^{(1)}$ . The difference is the new local current yield stress  $\sigma_{yc}^{(2)}$ .
5. Using the yield stress distribution  $\sigma_{yc}^{(2)}$ , perform a limit analysis using the constant primary loads. The limit load indicates a lower bound to the allowable constant load that will ensure shakedown just at the ratchet boundary. Alternatively, if plastic collapse is shown not to occur for the actual cyclic load, then the structure will shake down to steady strain cycles under the given loads.

The sections that follow will show how to apply this procedure to beams and pipes. The proposed method can be understood as an implementation and extension of the principle enunciated by Ponter and Karadeniz [8,9] that shakedown occurs if the plastic parts of the structure are cut away and the remaining parts shake down to elastic action.

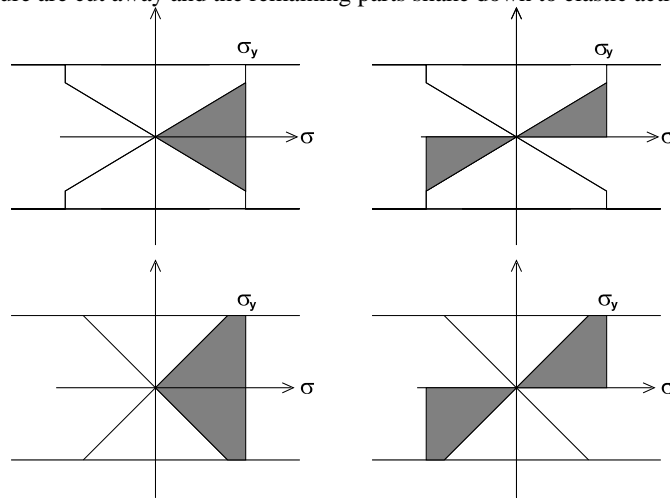


**Figure 1: Beam at ratchet boundary with given (secondary) cyclic load. shaded areas indicate stress available to support a time-invariant primary load. top row: cyclic load exceeding yield, bottom row: cyclic load below yield. left column: primary membrane, right column: primary bending.**

## SHAKEDOWN BOUNDARY FOR BEAMS UNDER MEMBRANE OR BENDING LOAD

The concepts of the previous section are now being used to examine beams under cyclic secondary bending and a constant primary load. The primary load is either axial or bending. For these cases, an analytical solution can be derived. One class of such problems are the Bree [10]-type problems, where cyclic secondary bending occurs with a constant primary membrane stress. In piping, this corresponds to secondary loads interacting with pressure-induced loads. Secondly consider cyclic secondary bending interacting with primary bending. In piping, this could mean bending from deadweight loading interacting with cyclic thermal bending of the pipe. Combinations of the foregoing two cases need to be considered as well.

For illustration purposes, the case of a rectangular beam is solved first due to its simplicity. The case of a piping cross section is addressed subsequently. A detailed derivation of the cases discussed below can be found in [11].

### Rectangular Beam

#### Primary Membrane and Cyclic Secondary Bending Loading

This is equivalent to the case underlying the Bree diagram [10]. Use of the present method is illustrated in Figure 1. The left two sketches address primary membrane and cyclic secondary bending loading. The three-step procedure is:

1. Determine the secondary stress amplitude as obtained from an elastic-plastic analysis with yield stress  $\sigma_y$ . This amplitude at the two extreme points of the cycle is indicated in Figure 1.
2. Choose the positive stress portions of the two extremes (thought of as occurring simultaneously) and subtract them from a uniform yield stress across the section. The result is the shaded area.

3. The shaded area, integrated across the section, gives the maximum membrane load that the section can support. The corresponding membrane stress is this load divided by the cross sectional area.

This process delivers the relationship between the applied cyclic secondary bending and the constant primary membrane load that the section can support without starting to ratchet. Two different cases can be distinguished depending on whether the secondary stress amplitude exceeds yield or not (The top sketch in Figure 1 depicts the case where yield is exceeded, the bottom sketch shows the case when yield is not exceeded).

When the secondary stress amplitude remains below the (cyclic) yield limit, the largest average primary membrane stress,  $\sigma_{pm}$ , that the section can support without ratcheting is

$$\sigma_{pm} = \sigma_y \left( 1 - \frac{1}{4} \frac{\Delta\sigma_{sb}}{\sigma_y} \right) \quad (1)$$

This expression is identical with the equation for the boundary between the elastic shakedown and the ratchet region in the Bree diagram [10] when  $\Delta\sigma_{sb}$  is less than  $2\sigma_y$ .

For the case of  $\Delta\sigma_{sb} \geq 2\sigma_y$ , the boundary between the ratcheting and the cyclic plasticity region is

$$\sigma_{pm} = \frac{\sigma_y^2}{\Delta\sigma_{sb}} \quad (2)$$

This last expression is again identical with the ratchet boundary of the Bree diagram [10]. The conclusion is that the present method recovers the ratchet boundary of the Bree diagram entirely, confirming the method works correctly.

Note that the method does not claim that the derived stress distributions have a specific relationship with the actual stress distributions during the cycle that would be seen when applying the combined primary and secondary loads. However, the claim is that the present procedure gives the same loads when integrated over the section.

#### *Primary Bending and Cyclic Secondary Bending Loading*

The following addresses the case where a constant primary bending load coexists with a secondary cyclic bending load. The present method is again illustrated in Figure 1. The right two sketches address primary bending and cyclic secondary bending loading. The basic procedure has three steps:

1. Determine the secondary stress amplitude as obtained from an elastic-plastic analysis with yield stress  $\sigma_y$ . This amplitude at the two extreme points of the cycle is indicated in Figure 1.
2. Choose the positive stress portions of the two extremes (thought of as occurring simultaneously) and subtract them from a uniform yield stress across the section. The result is the shaded area.
3. Calculate the bending moment of the shaded area. This gives the maximum primary bending load that the section can support. The corresponding bending stress is this load divided by the (elastic) section modulus,  $wh^2/6$ .

This process delivers the relationship between the applied cyclic secondary bending and the constant primary bending load that the section can support without starting to ratchet. Two different cases need to be distinguished depending on whether the secondary stress amplitude exceeds yield or not (The top sketch in Figure 1 depicts the case where yield is exceeded, the bottom sketch the case when yield is not exceeded).

When the secondary stress amplitude remains below the yield stress, the largest average primary bending stress,  $\sigma_{pb}$ , that the section can support without ratcheting is

$$\sigma_{pb} = \sigma_y \left( \frac{3}{2} - \frac{1}{2} \frac{\Delta\sigma_{sb}}{\sigma_y} \right) \quad (3)$$

When the cross section is partly yielding under the action of secondary cycling ( $\Delta\sigma_{sb} \geq 2\sigma_y$ ), the following expression describes the boundary between the ratcheting and the cyclic plasticity region.

$$\sigma_{pb} = 2\sigma_y \left( \frac{\sigma_y}{\Delta\sigma_{sb}} \right)^2 \quad (4)$$

Figure 2 shows a comparison of the ratchet boundary for primary membrane as compared to primary bending load. In both cases, cyclic plasticity can occur if the elastically calculated stress is below  $0.5\sigma_y$ . However, the beam can support a smaller bending than membrane stress in this region. The ratchet boundary is seen to be much steeper in the case of primary bending. Conversely, in terms of the elastic stress the bending capacity of the beam is above the capacity for membrane stress when the secondary cycling is below yield. The presently derived relationships are confirmed in [11]

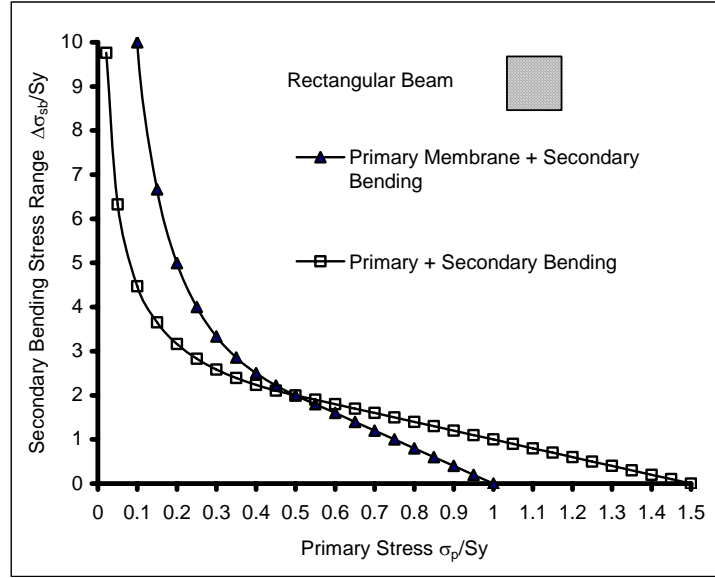


**Figure 2: Ratchet boundary for a rectangular beam subjected to cyclic secondary bending coincident with constant primary membrane (Bree problem) and with constant primary bending stress.**

#### *Primary Membrane Plus Bending and Cyclic Secondary Bending Loading*

The case where both time-invariant primary membrane and primary bending loads coexist with secondary cyclic bending is best studied by using the above solutions for the individual primary loads to normalize the respective simultaneous primary loads. Thus, an “interaction diagram” between primary membrane and bending loads is obtained that is analogous to the diagram for limit loads under combined membrane and bending loads. With  $\sigma_{pmi}$  and  $\sigma_{pbi}$  denoting the simultaneously applied loads, and  $\sigma_{mL}$  and  $\sigma_{bL}$  standing for the limit loads under the individual application of a membrane / bending load, the well known interaction formula for combined loading is

$$\frac{\sigma_{pbi}}{\sigma_{bL}} = 1 - \left( \frac{\sigma_{pmi}}{\sigma_{mL}} \right)^2 \quad (5)$$

Using the integration process described in [11], the interaction formula for the case where the cyclic load causes outer-fibre yielding ( $\Delta\sigma_{sb} \geq 2\sigma_y$ )

$$\frac{\sigma_{pbi}}{\sigma_{pb}} = 3 \left( 1 - \left( \frac{\sigma_{pmi}}{\sigma_{pm}} \right) \right) - 2 \sqrt{1 - \left( \frac{\sigma_{pmi}}{\sigma_{pm}} \right)^2}^3 \quad (6)$$

where  $\sigma_{pb}$  and  $\sigma_{pm}$  are from eq. (2) and (4), respectively. Note that this interaction formula is independent of the secondary stress range. This dependency is introduced only through  $\sigma_{pb}$  and  $\sigma_{pm}$ .

When there is no outer fibre yielding ( $\Delta\sigma_{sb} \leq 2\sigma_y$ ), the interaction formula becomes a weighted average between eq. (5) and (6), with the limit formula (5) reached when the secondary stress range  $\Delta\sigma_{sb} = 0$ , as expected.

$$\frac{\sigma_{pbi}}{\sigma_{pb}} = \frac{\Delta\sigma_{sb}}{2\sigma_y} \left[ 3 \left( 1 - \left( \frac{\sigma_{pmi}}{\sigma_{pm}} \right) \right) - 2 \sqrt{1 - \left( \frac{\sigma_{pmi}}{\sigma_{pm}} \right)^2}^3 \right] + \frac{2\sigma_y - \Delta\sigma_{sb}}{2\sigma_y} \left[ 1 - \left( \frac{\sigma_{pmi}}{\sigma_{mL}} \right)^2 \right] \quad (7)$$

#### **Pipe Cross Section**

The relationships for a pipe cross section can be derived in an analogous manner as those derived for the rectangular beam. The sketches shown in Figure 1 apply unchanged. However, the relationships will be more complicated because the cross section changes with the  $y$  coordinate, so that the proper integration over the section needs to be carried out to derive the quantities needed for the present analysis.

*Primary Membrane and Cyclic Secondary Bending Loading*

As in the case of a rectangular beam, the distinction between the cyclic secondary stress range below and above  $2 \sigma_y$  needs to be made. The following relationship applies to the case of  $\Delta\sigma_{sb} \leq 2 \sigma_y$ .

$$\sigma_{pm} = \sigma_y \left( 1 - \frac{\Delta\sigma_{sb}}{\sigma_y} \frac{1 - \frac{h}{R_o} + \frac{1}{3} \left( \frac{h}{R_o} \right)^2}{\pi \left( 1 - \frac{1}{2} \frac{h}{R_o} \right)} \right) \quad (8)$$

where  $h$  is the wall thickness, and  $R_o$  is the outer radius. The definitions of  $\Delta\sigma_{sb}$ ,  $\sigma_{pm}$  and  $\sigma_y$  are as before. As in the case of the rectangular cross section, this is the equation of a straight line in the Bree-type diagram.

When  $\Delta\sigma_{sb} \geq 2 \sigma_y$ , the applicable relationship is

$$\sigma_{pm} = \frac{\sigma_y}{\pi \frac{h}{R_o} \left( 1 - \frac{1}{2} \frac{h}{R_o} \right)} \left( \frac{\frac{2 \sigma_y}{\Delta\sigma_{sb}} \left( \sqrt{1 - \left( \frac{2 \sigma_y}{\Delta\sigma_{sb}} \right)^2} - \sqrt{\max \left( \left( 1 - \frac{h}{R_o} \right)^2 - \left( \frac{2 \sigma_y}{\Delta\sigma_{sb}} \right)^2, 0} \right)} + \arcsin \left( \frac{2 \sigma_y}{\Delta\sigma_{sb}} \right)} - \frac{\arcsin \left( \min \left( \frac{1}{1 - \frac{h}{R_o}}, \frac{2 \sigma_y}{\Delta\sigma_{sb}}, 1 \right) \right)}{\left( 1 - \frac{h}{R_o} \right)^2} + \frac{\Delta\sigma_{sb}}{3 \sigma_y} \left( \frac{\sqrt{1 - \left( \frac{2 \sigma_y}{\Delta\sigma_{sb}} \right)^2}}{-\sqrt{\max \left( \left( 1 - \frac{h}{R_o} \right)^2 - \left( \frac{2 \sigma_y}{\Delta\sigma_{sb}} \right)^2, 0} \right)}} \right)^3 \right) \quad (9)$$

The point at which  $\Delta\sigma_{sb} = 2 \sigma_y$  occurs at  $\sigma_{pm} < 0.5 \sigma_y$ . Figure 3(a) confirms that the pipe cross section with a realistic wall thickness to OD ratio will have a lower relative load capacity than the rectangular section.

*Primary Bending and Cyclic Secondary Bending Loading*

The relationship that applies to the case of  $\Delta\sigma_{sb} \leq 2 \sigma_y$  is

$$\sigma_{pb} = \sigma_y \left( \frac{16 \left( R_o^3 - (R_o - h)^3 \right) R_o}{3 \pi R_o^4 - (R_o - h)^4} - \frac{\Delta\sigma_{sb}}{2 \sigma_y} \right) \quad (10)$$

where  $h$  is the wall thickness, and  $R_o$  is the outer radius. The definitions of  $\Delta\sigma_{sb}$ ,  $\sigma_{pm}$  and  $\sigma_y$  are as before. At  $\Delta\sigma_{sb} = 2 \sigma_y$ , the primary bending stress that can be supported without ratcheting is  $\sigma_{pb} = (\zeta - 1) \sigma_y$ , where  $\zeta$  is the shape factor. For realistic pipe wall thicknesses this point lies therefore again below the corresponding value of  $0.5 \sigma_y$  for the rectangular section (which, as should be noted, is also at  $(\zeta - 1) \sigma_y$  for the rectangular section). Furthermore, the corresponding point for primary membrane loading occurs at a different stress value, unlike for the rectangular section where both points are at  $0.5 \sigma_y$ .

When  $\Delta\sigma_{sb} \geq 2 \sigma_y$ , the applicable relationship is

$$\sigma_{pb} = \frac{4 \sigma_y}{\pi \left( 1 - \left( 1 - \frac{h}{R_o} \right)^4 \right)} \left( \frac{\frac{4}{3} \left( 1 - \left( 1 - \frac{h}{R_o} \right)^3 \right) - \left( \frac{5}{6} - \frac{1}{3} \left( \frac{2 \sigma_y}{\Delta\sigma_{sb}} \right)^2 \right) \sqrt{1 - \left( \frac{2 \sigma_y}{\Delta\sigma_{sb}} \right)^2}}{-\frac{\Delta\sigma_{sb}}{4 \sigma_y} \left[ \arcsin \left( \frac{2 \sigma_y}{\Delta\sigma_{sb}} \right) - \left( 1 - \frac{h}{R_o} \right)^4 \arcsin \left( \min \left( \frac{1}{1 - \frac{h}{R_o}}, \frac{2 \sigma_y}{\Delta\sigma_{sb}}, 1 \right) \right) \right]} + \left( \frac{5}{6} \left( 1 - \frac{h}{R_o} \right)^2 - \frac{1}{3} \left( \frac{2 \sigma_y}{\Delta\sigma_{sb}} \right)^2 \right) \sqrt{\max \left( \left( 1 - \frac{h}{R_o} \right)^2 - \left( \frac{2 \sigma_y}{\Delta\sigma_{sb}} \right)^2, 0 \right)} \right) \quad (11)$$

Figure 3(b) shows again that the pipe cross section with a realistic wall thickness to OD ratio will have a lower relative load capacity than the rectangular section.

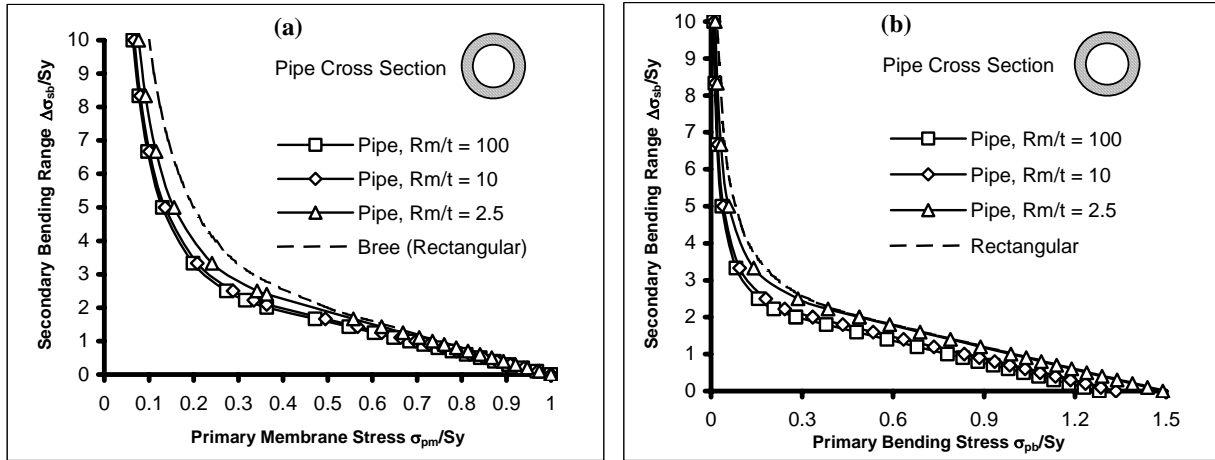


**Figure 3: Ratchet boundary for a straight pipe subjected to cyclic secondary bending coincident with (a) constant primary membrane stress and (b) constant primary bending stress.**

#### Primary Membrane Plus Bending and Cyclic Secondary Bending Loading

When a time-invariant primary membrane and bending load occurs simultaneously with cyclic bending, an interaction diagram for the primary loads can again be derived by integration of the difference between the yield stress and the cyclic stress amplitude. The integration extends from the outer fibre to some intermediate location for bending and over the remainder of the section to obtain the simultaneously supported force. Due to the shape of the cross section, the interaction curve will depend on the secondary stress level, even for cycling above yield, where the rectangular cross section had an invariant interaction curve. Due to the complicated shape, the exact relationship between the primary membrane and primary bending stress at a given secondary stress level can only be obtained as two fairly lengthy equations that contain a common parameter. At high levels of secondary stress, the equation becomes identical with that for the rectangular section, while near  $\Delta\sigma_{sb} = 2\sigma_y$ , it deviates slightly from this curve.

When the secondary cycling is below the yield level, the interaction curve is again obtained by linear interpolation between the curve at  $\Delta\sigma_{sb} = 2\sigma_y$  and the limit interaction curve as in eq. (7). The exact limit interaction curve can only be obtained in parametric form, but for realistic pipe sections, it is represented with excellent accuracy by the simple relationship

$$\frac{\sigma_{pbi}}{\sigma_{bL}} = \cos\left(\frac{\pi \sigma_{pmi}}{2 \sigma_{mL}}\right) \quad (12)$$

Not much would be gained by listing the exact equations for the interaction curves here. Figure 4 shows that the curves are all fairly close, and that the limit curve, eq. (12), is a lower bound for the load carrying capacity. Reference [11] contains examples to validate the relationships of eq. (8) to (11). Additionally, several points on the interaction curve were confirmed with cyclic analysis results for the present paper. Agreement to within about 5% with the present solution was corroborated.

## NUMERICAL IMPLEMENTATION

In piping analysis, it is customary to idealize the piping system as beams and then perform the evaluation using the moments derived from the beam model, as well as the pressure stress. The numerical implementation is therefore targeted to the use of beam elements as would be available in general-purpose finite element (FE) software.

The loading in a piping system is generally taken to be bending-dominated, where bending acts together with the pressure induced membrane stress. Accordingly, the present evaluation considers a cyclic bending load (which could, for example, be caused by the action of thermal loads) acting together with a time-invariant load that is either primary membrane (e.g. due to pressure) or primary bending, e.g. deadweight.

In the numerical implementation of the non-cyclic shakedown evaluation, the concept is to adjust the properties of the beam element to simulate a loss of load carrying capacity due to the presence of the cyclic stress. Only a single type of constant primary load will be considered to act during the cycle; therefore it is sufficient to adjust the yield stress as a single parameter. However, the adjustment will be different depending on the type of the primary load, i.e. whether it is a membrane or a bending load.

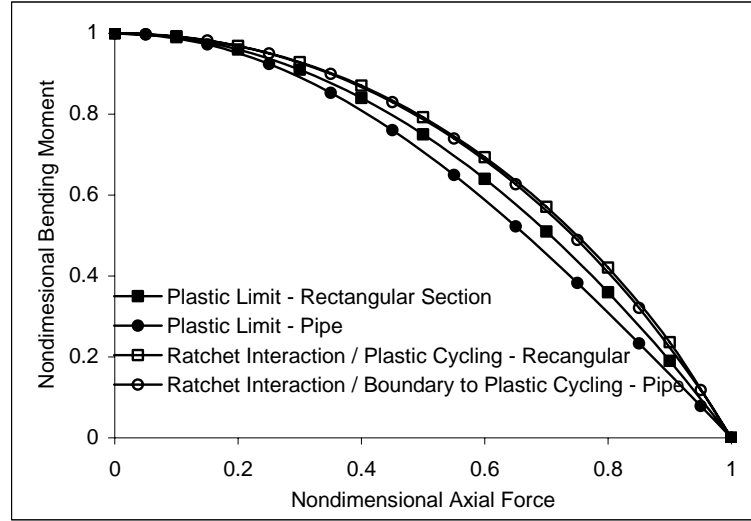


**Figure 4: Plastic limit and ratchet interaction diagram for rectangular beam and pipe. Primary axial force and primary bending moment are normalized with maximum load that the section will support when acting by itself.**

The proposed method proceeds in the following steps:

1. Model the piping system using the appropriate elastic-plastic beam elements. Set the yield stress to  $1.5 S_m$  and assume perfect plasticity.
2. Apply half the cyclic load range and obtain the bending moment distribution in the system and solve.
3. Use the local (nodal) bending moments and the fully plastic moment to adjust the yield stress of each element in the model for a subsequent FE run.
4. Using the modified model, perform a second run that applies the primary load that remains constant during the considered cycle. If a solution can be obtained (no plastic collapse), then shakedown is assured. To obtain the ratchet boundary, increase the primary load until limit collapse of the modified model occurs. This is the maximum primary load that can occur simultaneously with the given cyclic load without causing ratcheting.

The yield stress adjustment in step 3 is performed by using the bending moment in each elastic-plastic beam element after the step 2 run has been completed. At each node, the local moment  $M$  is obtained. The fully plastic (limit) beam moment,  $M_{pL}$ , is calculated and the ratchet boundary moment (primary moment at incipient ratchet),  $M_{pr}$ , is determined from

$$M_{pr} = M_{pL} - M \quad (13)$$

This moment is used to adjust the element parameters before the second run where only the time-invariant primary loads are applied. The adjustment procedure is as follows:

1. Using the nodal moment  $M$ , determine  $M_{pr}$  from eq. (13).
2. By employing the relationship  $M_{pr}/M_y = \sigma_{pb}/\sigma_y$  (where  $M_y$  is the elastic moment at the onset of yielding), solve the appropriate pipe equation, (10) or (11), for  $\Delta\sigma_{sb}/\sigma_y$ . For pipes, only a numerical solution is possible.
3. Substitute the obtained ratio  $\Delta\sigma_{sb}/\sigma_y$  into the appropriate expression for  $\sigma_{pm}$  from the previous Section, eq. (8) or (9). Calculate the ratchet boundary force,  $F_{pr}$ , from  $F_{pr} = \sigma_{pm} \pi R_o^2 (1-(h/R_o)^2)$ .
4. The yield stress and the outer radius of each element is now adjusted so that the limit loads of the model section match both the maximum force and moment that the section could support without ratcheting in the presence of the secondary load. The thickness to OD ratio is held constant. Therefore, the adjusted yield stress,  $\sigma_{y,adj}$ , and radius,  $R_{o,adj}$ , can be calculated from

$$\sigma_{y,adj} = \left( \frac{4}{3\pi} \right)^3 \frac{(1-(h/R_o)^3)^2}{(1-(h/R_o)^2)^3} \frac{F_{pr}^3}{M_{pr}^2}, \quad R_{o,adj} = \frac{3\pi}{4} \frac{1-(h/R_o)^2}{1-(h/R_o)^3} \frac{M_{pr}}{F_{pr}} \quad (14)$$

The described method will provide slightly conservative results for mixed membrane and bending primary loads, since it implies the use of the limit load interaction curve rather than the ratchet interaction curve for a section with cyclic secondary load. Due to the closeness of the interaction curves, this simplification is not considered as very detrimental. For a linear beam element, the lower of the two nodal adjusted yield stresses would be used for the element for additional conservatism. Adequate mesh refinement is needed to provide a good resolution of the bending moment gradients along the beam.

### Extension to General Piping Analysis

The extensions of the simple cases to a general piping analysis is envisioned as follows. Pressure loading must be addressed by using the hoop stress, rather than the axial stress together with the bending moments in evaluating shakedown, just like it is presently done in eq. (10) of NB-3600. This is recommended because the plastic flow rule, in particular the Tresca (maximum shear) rule, will relate stresses in different directions with each other.

The interaction of constant primary membrane and bending loads that occur simultaneously, like deadweight and pressure, is addressed here. Note also that piping systems may see a significant amount of torsion, which is currently combined with the components of bending moment, but which a more accurate evaluation might need to consider as a membrane stress.

For piping elements other than straight pipe, the present recommendation would be to use the appropriate stress indices for primary plus secondary loading ("C" indices) as defined in NB-3600 of Section III [4]. Specifically, for elbows, however, it has been noted by others [12] that the  $C_2$  indices for bending are probably conservative. Taking the non-local nature of ratcheting into account, Yang and Gurdal [12] concluded that a more realistic value of  $C_2$  should be at about 2/3 of the current Code value. This would put it in the neighbourhood of the  $B_2$  index, which may be understandable in the context of the present paper, which shows a very close relationship between the ratcheting boundary and plastic limit failure.

### CONCLUSIONS

A method to determine the ratchet boundary without the need for cyclic analysis has been developed. Using this method, the ratchet boundaries for simple scenarios that are relevant to piping analysis have been derived analytically. A numerical implementation applicable to beam models of a piping system has been constructed. The agreement between the theoretical solution and its numerical implementation has been good (within 5%).

Cyclic analysis confirms the theoretical predictions of the ratchet boundary in this paper with good accuracy. This shows that a close correspondence exists between the plastic limit load and ratcheting, and that ratcheting can be understood as an "incremental collapse". A "ratchet mechanism" needs to develop before ratcheting can occur in direct analogy to plastic collapse.

The non-cyclic method is considerably more computationally efficient than the cyclic method. To determine the ratchet boundary for a given cyclic load took about the same time as performing a single full cycle at a load level near that boundary. Therefore, if the cyclic analysis needs typically about 20 cycles to approximate steady state reasonably well, the non-cyclic method would require about 20 times less computation time. In addition, if the ratchet boundary needs to be established (as opposed to showing that a given level of the constant load is acceptable), several runs of the cyclic analysis would be needed (each to steady state). In this case, the non-cyclic method would have an even higher efficiency.

### REFERENCES

1. Bhagwagar, T., and Gurdal, R., "Straight Pipe Cyclic Analyses for Shakedown Verification Code Criteria", ASME PVP Vol. 453, ASME PVP Conference, Cleveland, OH, July 20-24, 2003, pp. 19-30.
2. Reinhardt, W., "A Non-Cyclic Method For Plastic Shakedown Analysis", ASME PVP-Vol. 458, ASME PVP Conference, Cleveland, OH, July 20-24, 2003, pp. 51-59.
3. Grandemange, J.M., Heliot, J, Vagner, J, Morel, A. and Faidy, C, "Improvements On Fatigue Analysis Methods For The Design Of Nuclear Components Subjected To The French RCC-M Code", WRC Bulletin 361, Welding Research Council, Shaker Heights OH, 1991, pp.1-12.
4. ASME Boiler and Pressure Vessel Code, American Society of Mechanical Engineers, New York, 2004.
5. Gokhfeld, D.A., and Cherniavsky, O.F., "Limit Analysis of Structures at Thermal Cycling", Sijthoff & Noordhoff, Alphen aan den Rijn, The Netherlands, 1980.
6. Reinhardt, W., 2003, "Distinguishing Ratcheting and Shakedown Conditions in Pressure Vessels", ASME PVP-Vol. 458, ASME PVP Conference, Cleveland, OH, July 20-24, 2003, pp.13-26.
7. Melan, E., "Zur Plastizität des räumlichen Kontinuums," Ingenieur-Archiv, Vol. 9(2), 1938, pp. 116-123.
8. Ponter, A.R.S., and Karadeniz, S., "An Extended Shakedown Theory for Structures that Suffer Cyclic Thermal Loading. Part I: Theory," ASME J. Appl. Mech., Vol. 52(4), 1985, pp. 877-882.
9. Ponter, A.R.S., and Karadeniz, S., "An Extended Shakedown Theory for Structures that Suffer Cyclic Thermal Loading. Part II: Applications," ASME J. Appl. Mech., Vol. 52(4), 1985, pp. 883-889.
10. Bree, J., "Elastic-Plastic Behaviour of Thin Tubes Subjected to Internal Pressure and Intermittent High-Heat Fluxes with Application to Fast-Nuclear-Reactor Fuel Elements," J. Strain Analysis, Vol. 2(3), 1967, pp. 226-238.
11. Reinhardt, W, "Elastic-Plastic Shakedown Assessment Of Piping Using A Non-Cyclic Method", PVP2007-26703, 2007 ASME PVP/ CREEP8 Conference, San Antonio, Texas, USA, July 22-26, 2007.
12. Yang, J., and Gurdal, R., "Piping Elbow Cyclic Analyses for Shakedown Verification", ASME PVP Vol. 453, ASME PVP Conference, Cleveland, OH, July 20-24, 2003, pp. 49-59.